Deterministic Generation of Loss-Tolerant Photonic Cluster States with a Single Quantum Emitter

Yuan Zhan and Shuo Sun*
JILA and Department of Physics, University of Colorado, Boulder, Colorado 80309, USA

(Received 6 July 2020; accepted 29 October 2020; published 24 November 2020)

A photonic cluster state with a tree-type entanglement structure constitutes an efficient resource for quantum error correction of photon loss. But the generation of a tree cluster state with an arbitrary size is notoriously difficult. Here, we propose a protocol to deterministically generate photonic tree states of arbitrary size by using only a single quantum emitter. Photonic entanglement is established through both emission and rescattering from the same emitter, enabling fast and resource-efficient entanglement generation. The same protocol can also be extended to generate more general tree-type entangled states.

DOI: 10.1103/PhysRevLett.125.223601

Photons are unique carriers of quantum information. They have multiple degrees of freedom that can be employed to carry either qubits or qudits. In addition, photons are immune from thermal noise at room temperature, capable of long-distance transmission, and barely interact with each other. These properties make them ideal for quantum communication [1–3] and quantum networking [4,5]. While the lack of photon-photon interactions makes them less appealing in gate-based quantum computing, optical quantum computers can be constructed using a cluster-state-based model, known as "measurement-based quantum computation" [6,7]. This model offers tremendous advantages for optical implementations since high-fidelity single-qubit gates and detectors can be realized with mature photonic devices [8,9].

A major obstacle in all these applications is the loss of photons during transmission, either in a quantum communication channel or in a delay line of an optical quantum computer. Imperfect quantum efficiency of single-photon detectors can also be accounted as loss. Photon loss poses an exponential trade-off between the rate and distance of repeaterless quantum communication in optical fibers [10], as well as a fundamental limit on the scalability of an optical quantum computer. It is thus essential to develop resource-efficient error correction methods that can deal with loss fault tolerantly [11–13].

One such approach is to encode a qubit in a highly entangled multiphoton cluster state, such as a tree cluster state [14,15]. The built-in redundancy in the tree-structure entanglement enables indirect measurement of a qubit even when a subset of the photons in the tree is lost [14]. Unfortunately, generating a multiphoton entangled state with such a complicated entanglement structure is extremely challenging. Standard approaches rely on pairwise fusion gates to grow entangled photon pairs into a multiphoton cluster state [16–19]. The probabilistic nature of the fusion gates leads to a tremendous overhead on the required resources and a slow generation rate (~mHz for 12-photon entanglement with state-of-the-art experiments [20]). To overcome this challenge, Lindner and Rudolph presented a deterministic protocol to generate multiphoton entangled states through sequential emission of photons from a single quantum emitter [21], but photons emitted in this process can only be entangled in the form of a one-dimensional chain. Inspired by this work, Buterakos *et al.* proposed a protocol that can sequentially emit photons into a repeater graph state with the help of an ancillary matter qubit [22]. While this protocol can be extended to generate a tree cluster state as shown in the same work, it requires as many ancillary matter qubits as the depth of the tree, along with the capability to perform two-qubit entangling gates between the quantum emitter and all the ancillary qubits. This demanding requirement limits the scale of the tree state that one can generate experimentally. In addition, since the entangling operation between the ancillary matter qubit and the quantum emitter is typically much slower than optical processes, the large number of entangling gates significantly reduces the generation rate of the tree state and the repeater graph state. In fact, it has been recently shown that the slow entangling operation between the matter qubits is the dominant limiting factor for the performance of the cluster-state-based all-optical quantum repeaters [23].

In this Letter, we propose a new protocol to deterministically generate a photonic tree state using only a single quantum emitter. The emitter is strongly coupled to a chiral waveguide that has a mirror at one end implementing a delayed feedback. The entanglement structure is thus established through both sequential emission of photons from the quantum emitter and rescattering of photons following the delayed feedback, enabling fast and resource-efficient generation of the tree cluster states.

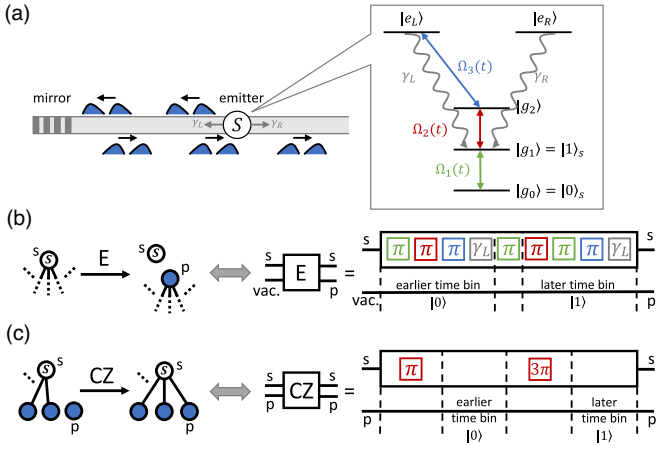

FIG. 1. (a) The schematic setup to generate a photonic tree cluster state with an arbitrary size. The inset shows the energy-level structure of the quantum emitter. (b),(c) The left-hand panels illustrate the effects of the E gate (b) and the CZ gate (c) applied on the joint emitter-photon quantum state. The right-hand panels show the pulse sequences required to implement the E gate (b) and the CZ gate (c). The color of each block in the pulse sequence is used to indicate the optical transition [also color labeled in (a)] to which the rotation pulse is applied.

While a similar scheme has been proposed to generate projected entangled pair states [24], our proposal for the first time shows the capability to generate complex aperiodic entanglement structures with a simple delayed feedback. We also analyze our protocol under realistic error models and show that the protocol is robust against typical errors associated with its potential experimental platforms. Our proposal paves the way toward the realization of all-optical quantum repeaters [12,13,18] and loss-tolerant optical quantum processors [11].

Figure 1(a) shows the schematic setup we propose to generate the photonic tree state. It consists of a single quantum emitter (labeled S), a chiral waveguide, and a distant mirror placed at one end of the waveguide. For concreteness, we assume the emitter has an energy-level structure as shown in the inset of Fig. 1(a). It consists of three metastable ground states, labeled as $|g_0\rangle$, $|g_1\rangle$, and $|g_2\rangle$. The states $|g_0\rangle$ and $|g_1\rangle$ form a stable qubit ($|0\rangle_s \equiv |g_0\rangle$ and $|1\rangle_s \equiv |g_1\rangle$), which can be coherently manipulated with a classical field $\Omega_1(t)$. The state $|g_2\rangle$ serves as an ancillary memory state used in the generation of time-bin encoded photons, as will be explained next. The population of this state can be coherently prepared from the state $|g_1\rangle$ with another classical field $\Omega_2(t)$. The quantum emitter also consists of two optically excited states $|e_L\rangle$ and $|e_R\rangle$. Both excited states can decay into the ground state $|g_1\rangle$ while emitting a photon into the waveguide. We assume the couplings between the emitter and the waveguide are chiral, such that the transitions $|g_1\rangle \leftrightarrow |e_L\rangle$ and $|g_1\rangle \leftrightarrow |e_R\rangle$ couple only to the left- and right-propagating modes of the waveguide, respectively. Such chiral couplings have been experimentally demonstrated across a number of atomic systems [25]. We assume that we can drive the emitter into the excited state $|e_L\rangle$ from the ancillary ground state $|g_2\rangle$ with an optical laser $\Omega_3(t)$.

We encode each photonic qubit in the time-bin basis consisting of two possible temporal modes well separated from each other. Specifically, we denote the presence of a photon in the earlier and later temporal modes as $|0\rangle_p$ and $|1\rangle_p$, respectively. The time-bin encoding is uniquely suitable for long-distance quantum communication [26], as it is robust to depolarization errors and also allows for the detection of photon loss.

We first introduce the two elementary gates required to implement our protocol, the E gate and the controlled-Z (CZ) gate. The left-hand panel in Fig. 1(b) illustrates the action of the E gate on the joint emitter-photon quantum state. An E gate generates a new photon that inherits the state of the quantum emitter, while resetting the state of the quantum emitter to $|1\rangle_s$. Mathematically, the transformation of the E gate can be written as $(\alpha|0\rangle_s|\psi_0\rangle_r + \beta|1\rangle_s|\psi_1\rangle_r)|\text{vacuum}\rangle_p \rightarrow (\alpha|0\rangle_p|\psi_0\rangle_r + \beta|1\rangle_p|\psi_1\rangle_r)|1\rangle_s$, where s, r, and p represent the states of the emitter, the rest of the photons that are already emitted which may be entangled with the emitter, and the newly generated photon, respectively. The right-hand panel in Fig. 1(b) shows the pulse sequence required to implement the E gate. By successively applying three π pulses of $\Omega_1(t)$, $\Omega_2(t)$, and $\Omega_3(t)$, the emitter can be excited to state $|e_L\rangle$ and emits a left-propagating photon into the earlier time bin if it is initially in state $|g_0\rangle$, while populated to $|g_0\rangle$ if initially in $|g_1\rangle$. We next apply a π pulse of $\Omega_1(t)$ to swap $|g_0\rangle$ and $|g_1\rangle$, and repeat the process to generate a left-propagating photon into the later time bin if the emitter is initially in state $|g_1\rangle$. Another π pulse of $\Omega_1(t)$ is used to make sure that the emitter is reset to $|g_1\rangle$ regardless of its initial state. Figure 1(c) shows the action of the CZ gate on the joint emitter-photon quantum state, along with the required pulse sequence for its realization. The CZ gate is applied between the emitter and a photon reflected from the mirror. To implement the CZ gate, we apply a π pulse of $\Omega_2(t)$ before the earlier time bin, and another 3π pulse of $\Omega_2(t)$ in the middle of the earlier and later time bins. Therefore, if the photon is in the state $|1\rangle_p$ (later time bin), it will pick up a π phase shift if the emitter is initially in the state $|g_1\rangle$ due to the strong coupling between the transition $|g_1\rangle \leftrightarrow |e_R\rangle$ and the right-propagating mode of the waveguide [27,28], but no phase shift if the emitter is initially in the state $|g_0\rangle$. A photon in state $|0\rangle_p$ (earlier time bin) will always transmit with no phase shift since the emitter can only be in state $|g_0\rangle$ or $|g_2\rangle$ during the earlier time bin. The 3π rotation in the second $\Omega_2(t)$ pulse, instead of a π rotation, avoids accumulation of a π geometric phase between the emitter states $|g_0\rangle$ and $|g_1\rangle$.

To provide an intuitive understanding, we first describe our protocol using an example of a tree shown in Fig. 2(f),

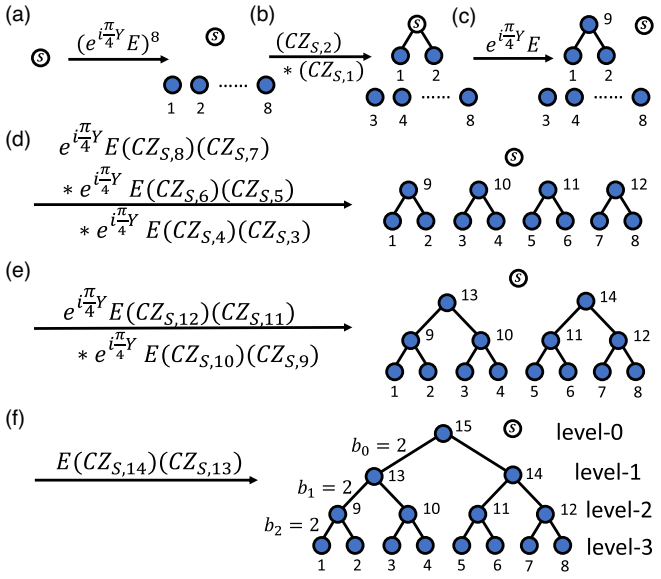

FIG. 2. Graph representation of the procedure for generating a tree with branching parameters $b_0 = b_1 = b_2 = 2$.

which has a depth of 3 and branching parameters of $b_0 = b_1 = b_2 = 2$. However, it should be noted that our protocol applies to any arbitrary tree structures and sizes. Here we define the branching parameter b_i as the number of leaf nodes connected with a node at level i, where the level number i is defined as the number of edges on the path from the node of interest to the root node of the tree. Our protocol generates photons from the bottom of the tree to the top, as shown by the graph representation of the procedure in Fig. 2. We start with the emitter prepared in state $|+\rangle_s = (1/\sqrt{2})(|0\rangle_s + |1\rangle_s)$. By continuously applying the E gate and a $(-\pi/2)$ spin rotation along the y axis of the Bloch sphere for 8 times, we generate 8 photons that are all in the state $|+\rangle_p = (1/\sqrt{2})(|0\rangle_p + |1\rangle_p)$ [see Fig. 2(a)]. These photons will constitute the bottom layer of the tree. The 8 photons will travel sequentially in the left-propagating mode of the waveguide until they are reflected by the mirror. For each reflected photon, we apply a CZ gate when the photon arrives at the emitter. Since both the emitter and the photon are in the superposition state, the CZ gate entangles the emitter and the photon. Therefore, after the first two photons pass through the emitter, the emitter will be entangled with both photons as shown in Fig. 2(b). Before the third photon arrives at the emitter, we apply an E gate to generate a new photon (the ninth photon) into the left-propagating mode of the waveguide. This E gate will transfer the state of the emitter into the ninth photon and reset the emitter to state $|1\rangle_s$. Thus the ninth photon becomes the parent node of the photons 1 and 2, and the emitter is detached from this subtree [see Fig. 2(c)]. A follow-up $(-\pi/2)$ rotation along the y axis on the emitter will prepare the emitter back to the $|+\rangle_s$ state again. Repeating the same procedure for another 3 times will generate three more subtrees, as shown in Fig. 2(d). Up to now, the photons 1–8 have passed through the emitter in the right-propagating mode and will no longer interact with the emitter, whereas the photons 9–12 are in the left-propagation mode of the waveguide and will be reflected back to the emitter. Following the same procedure, we will again entangle the emitter with both the photons 9 and 10 through two sequential CZ gates applied when they arrive at the emitter, and transfer the emitter state into another newly generated photon (the 13th photon) through an E gate. Repeating this procedure one more time will generate two larger subtrees, as shown in Fig. 2(e). Lastly, we will repeat the same procedure for the last time and generate the root node of the tree using an E gate (photon 15), which also decouples the emitter from the whole tree.

We now formalize our protocol for generating a general tree state with a depth of d and branching parameters $\{b_0, b_1, \ldots, b_{d-1}\}$. The sequence of operations can be described as follows:

$$|\psi_{\text{tree}}\rangle = \prod_{j=1}^{d}\left[\prod_{k=1}^{n_{d-j}}\left(e^{i(\pi/4)Y}E\prod_{l=1}^{b_{d-j}}\mathrm{CZ}_{S,\sum_{m=0}^{j-1}n_{d+1-m}+(k-1)b_{d-j}+l}\right)\right](e^{i(\pi/4)Y}E)^{n_d}|+\rangle_s, \tag{1}$$

where $n_l = \prod_{i=0}^{l-1} b_i$ is the number of photons in the lth level of the tree. $\mathrm{CZ}_{S,i}$ represents a CZ gate applied on the emitter S and the ith generated photon.

While we described our protocol using a specific system consisting of a multilevel atom coupled to a chiral waveguide, it is worth noting that neither the specific atomic level structure nor the chiral coupling is essential to the realization of our protocol. For example, our protocol can be realized with a cavity QED device with a simple II-type and Λ-type atom, as described in the Supplemental Material [29]. Such a cavity QED system has been realized by a number of atomic systems including trapped Rb atoms [37], semiconductor quantum dots [43,44], and diamond color centers [45].

We now discuss the robustness of our protocol against typical errors during the tree-state generation. One of the dominant errors in any photon generation process is the internal photon loss, which in our scheme may result from emission or rescattering of photons into the bath other than the waveguide mode due to the finite cooperativity,

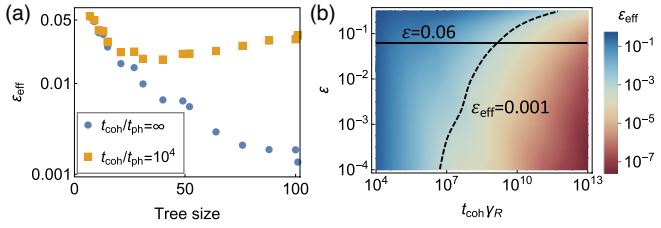

FIG. 3. (a) The effective error probability of the logic qubit encoded by the tree as a function of the tree size (the total number of photons in the tree). We assume a single-photon loss probability of $\varepsilon = 0.1$ in this calculation. The blue circles represent the case where $t_{\rm coh} \to \infty$, and the orange squares represent the case where $t_{\rm coh}/t_{\rm ph} = 10^4$. (b) The optimized value of $\varepsilon_{\rm eff}$ as a function of single-photon loss probability and coherence-time-bandwidth product.

absorption during photon transmission in the waveguide, and partial reflection from the end mirror. While the external loss is quantum error correctable due to the tree-type encoding, the internal loss may lead to uncorrectable errors since it happens before the tree entanglement is fully established. Following the proof shown in Ref. [14], we can show that the internal loss can be indeed corrected in the same way as the external photon loss. This is fundamentally because the attempted CZ gate operates as an identity operation when a photon is lost internally. Therefore, our protocol is loss resilient as long as the total loss is below the quantum error correction threshold of 50% [14]. As an example, we consider a specific application of performing an arbitrary single-qubit measurement on the tree-encoded logic qubit. We define the effective error probability $\varepsilon_{\rm eff}$ as the probability that this measurement yields an incorrect result. The blue circles in Fig. 3(a) show the value of $\varepsilon_{\rm eff}$ as a function of the total number of photons in the tree [29], with a single-photon loss probability of $\varepsilon = 0.1$. The effective error probability decreases exponentially with the tree size and can eventually approach 0 given a large enough tree.

While we can in principle overcome the photon loss by generating a large enough tree, in practice the size of the tree we can generate is limited by the finite coherence time of the emitter qubit. The orange squares in Fig. 3(a) show the effective error probability $\varepsilon_{\rm eff}$ when we consider a finite emitter coherence time $t_{\rm coh}$. Here we set $t_{\rm coh}/t_{\rm ph} = 10^4$ [29], where $t_{\rm ph}$ is the time allocated to a single-photon qubit. We have kept the same single-photon loss rate of $\varepsilon = 0.1$ in the calculation. As we can see from Fig. 3(a), when the tree size is small, the effective error probability is nearly identical with the value under infinite emitter qubit coherence time (blue circles), since the probability of emitter decoherence during the tree-state generation is negligible. However, as we keep increasing the tree size, the effective error probability tapers off and starts to increase, indicating that error caused by the emitter decoherence during the tree-state generation starts to dominate. Thus, given a qubit coherence time and single-photon loss rate, there is an optimized value of $\varepsilon_{\rm eff}$ that we can achieve by varying the tree size.

Figure 3(b) shows the optimized value of $\varepsilon_{\rm eff}$ at different system parameters [29]. In this calculation, we vary both the single-photon loss rate ε and the emitter qubit coherence time $t_{\rm coh}$, while assuming all other possible imperfections absent (see Supplemental Material [29] for a fidelity and error analysis when accounting for more experimental imperfections). We normalize $t_{\rm coh}$ in terms of the inverse of the bandwidth of the CZ gate γ_R, which is the waveguide modified linewidth of transition $|g_2\rangle \leftrightarrow |e_R\rangle$. As we can see, a small single-photon loss rate and a large coherence-time-bandwidth product $t_{\rm coh}\gamma_R$ are needed to achieve a small $\varepsilon_{\rm eff}$. To qualitatively identify the useful regime of $\varepsilon_{\rm eff}$, we consider a specific application of using tree states to implement one-way quantum repeaters [18,19,46]. We assume a realistic internal photon loss rate of 0.01, and we distribute the quantum repeater nodes one in every 1 km. This distance corresponds to an external photon loss rate of 0.05 in a telecom fiber, which is small enough compared with the threshold of 0.5 for loss correction, but large enough to ensure that dominant loss to be corrected is from the optical fiber. Since we have 10^3 repeater nodes, to achieve a reasonable communication rate over 1000 km requires the effective error probability of each link to be less than $\sim 10^{-3}$. The dashed line in Fig. 3(b) denotes the parameter regime where $\varepsilon_{\rm eff} = 10^{-3}$, and the solid line shows the condition where $\varepsilon = 0.06$, corresponding to the total loss rate of a single photon. Thus, to achieve $\varepsilon_{\rm eff} < 10^{-3}$ while $\varepsilon > 0.06$ requires a coherence-time-bandwidth product exceeding 10^9. This parameter regime can possibly be achieved upon reasonable improvements by using a single silicon-vacancy color center coupled with a photonic crystal cavity ($\gamma_R \sim 2\pi \times 10$ GHz [42] and $t_{\rm coh} \sim 10$ ms [38]), or a single trapped atom strongly coupled with a fiber Fabry-Perot cavity ($\gamma_R \sim 2\pi \times 100$ MHz [47] and $t_{\rm coh} \sim 1$ s [37]). It may also be possible to use a strongly coupled quantum dot and nanocavity ($\gamma_R \sim 2\pi \times 80$ GHz [39]) to reach this parameter regime, if one can improve its spin coherence time to ~ 2 ms (currently it is ~ 4 μs [48]).

In conclusion, we have proposed and analyzed a protocol for deterministic generation of tree-type photonic cluster states using only a single quantum emitter. Our protocol can generate a tree state with an arbitrary size and depth without any probabilistic fusion gates or ancillary matter qubits, which significantly reduces the resource overhead required for the entanglement generation. The protocol is also robust to typical errors in realistic experiments and is within reach upon reasonable improvements of quantum photonics technologies. In addition, our scheme can be implemented with a variety of cavity QED systems using both free-space optics and integrated photonics [29].

One of the most important features of our protocol is that it can be widely applicable to a large range of tree-type photonic cluster states that are useful for all-optical quantum repeaters, such as the repeater graph states [18,19] and the tree-encoded repeater graph states [19,22] (see Supplemental Material for details [29]). Thus, an important future work is to perform quantitative rate-distance trade-off and resource cost analysis of our scheme in the application of different all-optical quantum repeater protocols by accounting for all possible losses, bit flips, and dephasing errors, and systematically compare its performance with existing cluster state generation schemes [19,23,46]. Overall, our results constitute an important scheme for aperiodic 2D cluster state generation with feasible resources and pave the way toward the realization of loss-tolerant one-way optical quantum computers [11] and all-optical quantum repeaters [12,13,18].

We thank Paul Hilaire, Sophia Economou, and Edwin Barnes for fruitful discussions, and Chao-Yang Lu and Stefano Pirandola for useful input. We acknowledge funding from NSF (Grant No. PHYS 1734006).

*shuosun@jila.colorado.edu

[1] N. Sangouard, C. Simon, H. de Riedmatten, and N. Gisin, Rev. Mod. Phys. **83**, 33 (2011).
[2] T. E. Northup and R. Blatt, Nat. Photonics **8**, 356 (2014).
[3] F. Xu, X. Ma, Q. Zhang, H.-K. Lo, and J.-W. Pan, Rev. Mod. Phys. **92**, 025002 (2020).
[4] H. J. Kimble, Nature (London) **453**, 1023 (2008).
[5] S. Wehner, D. Elkouss, and R. Hanson, Science **362**, eaam9288 (2018).
[6] R. Raussendorf and H. J. Briegel, Phys. Rev. Lett. **86**, 5188 (2001).
[7] M. A. Nielsen, Phys. Rev. Lett. **93**, 040503 (2004).
[8] P. Kok, W. J. Munro, K. Nemoto, T. C. Ralph, J. P. Dowling, and G. J. Milburn, Rev. Mod. Phys. **79**, 135 (2007).
[9] J. L. O'Brien, Science **318**, 1567 (2007).
[10] S. Pirandola, R. Laurenza, C. Ottaviani, and L. Banchi, Nat. Commun. **8**, 15043 (2017).
[11] M. A. Nielsen and C. M. Dawson, Phys. Rev. A **71**, 042323 (2005).
[12] L. Jiang, J. M. Taylor, K. Nemoto, W. J. Munro, R. Van Meter, and M. D. Lukin, Phys. Rev. A **79**, 032325 (2009).
[13] S. Muralidharan, J. Kim, N. Lütkenhaus, M. D. Lukin, and L. Jiang, Phys. Rev. Lett. **112**, 250501 (2014).
[14] M. Varnava, D. E. Browne, and T. Rudolph, Phys. Rev. Lett. **97**, 120501 (2006).
[15] M. Varnava, D. E. Browne, and T. Rudolph, Phys. Rev. Lett. **100**, 060502 (2008).
[16] D. E. Browne and T. Rudolph, Phys. Rev. Lett. **95**, 010501 (2005).
[17] C.-Y. Lu, W.-B. Gao, J. Zhang, X.-Q. Zhou, T. Yang, and J.-W. Pan, Proc. Natl. Acad. Sci. U.S.A. **105**, 11050 (2008).
[18] K. Azuma, K. Tamaki, and H.-K. Lo, Nat. Commun. **6**, 6787 (2015).
[19] M. Pant, H. Krovi, D. Englund, and S. Guha, Phys. Rev. A **95**, 012304 (2017).
[20] H.-S. Zhong, Y. Li, W. Li, L.-C. Peng, Z.-E. Su, Y. Hu, Y.-M. He, X. Ding, W. Zhang, H. Li, L. Zhang, Z. Wang, L. You, X.-L. Wang, X. Jiang, L. Li, Y.-A. Chen, N.-L. Liu, C.-Y. Lu, and J.-W. Pan, Phys. Rev. Lett. **121**, 250505 (2018).
[21] N. H. Lindner and T. Rudolph, Phys. Rev. Lett. **103**, 113602 (2009).
[22] D. Buterakos, E. Barnes, and S. E. Economou, Phys. Rev. X **7**, 041023 (2017).
[23] P. Hilaire, E. Barnes, and S. E. Economou, arXiv:2005.07198.
[24] H. Pichler, S. Choi, P. Zoller, and M. D. Lukin, Proc. Natl. Acad. Sci. U.S.A. **114**, 11362 (2017).
[25] P. Lodahl, S. Mahmoodian, S. Stobbe, A. Rauschenbeutel, P. Schneeweiss, J. Volz, H. Pichler, and P. Zoller, Nature (London) **541**, 473 (2017).
[26] J. Brendel, N. Gisin, W. Tittel, and H. Zbinden, Phys. Rev. Lett. **82**, 2594 (1999).
[27] E. Waks and J. Vuckovic, Phys. Rev. Lett. **96**, 153601 (2006).
[28] S. Fan, Ş. E. Kocabaş, and J.-T. Shen, Phys. Rev. A **82**, 063821 (2010).
[29] See Supplemental Material at http://link.aps.org/supplemental/10.1103/PhysRevLett.125.223601 for details of alternative experimental implementations, fidelity and error analysis, effective error probability calculations, and the process to generate other photonic cluster states with tree-type entanglement structures, which includes Refs. [14,18,19,22–24,30–42].
[30] M. Hennrich, T. Legero, A. Kuhn, and G. Rempe, Phys. Rev. Lett. **85**, 4872 (2000).
[31] A. Kuhn, M. Hennrich, and G. Rempe, Phys. Rev. Lett. **89**, 067901 (2002).
[32] M. Hein, J. Eisert, and H. J. Briegel, Phys. Rev. A **69**, 062311 (2004).
[33] D. Walls and G. Milburn, *Quantum Optics* (Springer, Berlin, 2007).
[34] K. De Greve, L. Yu, P. L. McMahon, J. S. Pelc, C. M. Natarajan, N. Y. Kim, E. Abe, S. Maier, C. Schneider, M. Kamp, S. Höfling, R. H. Hadfield, A. Forchel, M. M. Fejer, and Y. Yamamoto, Nature (London) **491**, 421 (2012).
[35] A. Reiserer, N. Kalb, G. Rempe, and S. Ritter, Nature (London) **508**, 237 (2014).
[36] T. M. Sweeney, S. G. Carter, A. S. Bracker, M. Kim, C. S. Kim, L. Yang, P. M. Vora, P. G. Brereton, E. R. Cleveland, and D. Gammon, Nat. Photonics **8**, 442 (2014).
[37] A. Reiserer and G. Rempe, Rev. Mod. Phys. **87**, 1379 (2015).
[38] D. D. Sukachev, A. Sipahigil, C. T. Nguyen, M. K. Bhaskar, R. E. Evans, F. Jelezko, and M. D. Lukin, Phys. Rev. Lett. **119**, 223602 (2017).
[39] Y. Ota, D. Takamiya, R. Ohta, H. Takagi, N. Kumagai, S. Iwamoto, and Y. Arakawa, Appl. Phys. Lett. **112**, 093101 (2018).
[40] S. Sun, J. L. Zhang, K. A. Fischer, M. J. Burek, C. Dory, K. G. Lagoudakis, Y.-K. Tzeng, M. Radulaski, Y. Kelaita, A. Safavi-Naeini, Z.-X. Shen, N. A. Melosh, S. Chu, M. Lončar, and J. Vučković, Phys. Rev. Lett. **121**, 083601 (2018).

[41] D. Najer, I. Söllner, P. Sekatski, V. Dolique, M. C. Löbl, D. Riedel, R. Schott, S. Starosielec, S. R. Valentin, A. D. Wieck, N. Sangouard, A. Ludwig, and R. J. Warburton, Nature (London) **575**, 622 (2019).

[42] M. K. Bhaskar, R. Riedinger, B. Machielse, D. S. Levonian, C. T. Nguyen, E. N. Knall, H. Park, D. Englund, M. Lončar, D. D. Sukachev, and M. D. Lukin, Nature (London) **580**, 60 (2020).

[43] P. Lodahl, S. Mahmoodian, and S. Stobbe, Rev. Mod. Phys. **87**, 347 (2015).

[44] S. Sun, H. Kim, G. S. Solomon, and E. Waks, Nat. Nanotechnol. **11**, 539 (2016).

[45] A. Sipahigil, R. E. Evans, D. D. Sukachev, M. J. Burek, J. Borregaard, M. K. Bhaskar, C. T. Nguyen, J. L. Pacheco, H. A. Atikian, C. Meuwly, R. M. Camacho, F. Jelezko, E. Bielejec, H. Park, M. Lončar, and M. D. Lukin, Science **354**, 847 (2016).

[46] J. Borregaard, H. Pichler, T. Schröder, M. D. Lukin, P. Lodahl, and A. S. Sørensen, Phys. Rev. X **10**, 021071 (2020).

[47] M. Brekenfeld, D. Niemietz, J. D. Christesen, and G. Rempe, Nat. Phys. **16**, 647 (2020).

[48] L. Huthmacher, R. Stockill, E. Clarke, M. Hugues, C. Le Gall, and M. Atatüre, Phys. Rev. B **97**, 241413(R) (2018).